coatings

Supplementary Materials: Structural Evaluation of Coal-Tar-Pitch-Based Carbon Materials and their Na^+ Storage Properties

Ruilin Yin [1], Kun Wang [1,*], Beibei Han [2], Guiying Xu [1,*], Lixiang Li [1], Baigang An [1], Dongying Ju [2], Maorong Chai [2], Songnan Li [3] and Weimin Zhou [1,*]

[1] Key Laboratory of Energy Materials and Electrochemistry Research Liaoning Province, University of Science and Technology Liaoning, Anshan 114051, China; lin13050079658@163.com (R.Y.); lxli2005@126.com (L.L.); baigang73@126.com (B.A.)
[2] Advanced Science Research Laboratory, Saitama Institute of Technology, Fusaiji 1690, Fukaya, Japan; hanbeibei@nimte.ac.cn (B.H.); dyju@sit.ac.jp (D.J.); chaimaorong@spic.com.cn (M.C.)
[3] JiXi Weida New Material Technology Co., Ltd, Jixi 158100, China; aabbcc_2000@126.com
* Correspondence: wk172860@ustl.edu.cn (K.W.); xuguiying751107@ustl.edu.cn (G.X.); aszhou@ustl.edu.cn (W.Z.)

Citation: Yin, R.; Wang, K.; Xu, G.; An, B.; Ju, D.; Chai, M.; Li, S.; Zhou, W. Structural Evaluation of Coal-Tar-Pitch-Based Carbon Materials and their Na^+ Storage Properties. *Coatings* **2021**, *volume number*, x. https://doi.org/10.3390/coatings11080948

Academic Editor(s): Je Moon Yun

Received: 17 June 2021
Accepted: 2 August 2021
Published: 8 August 2021

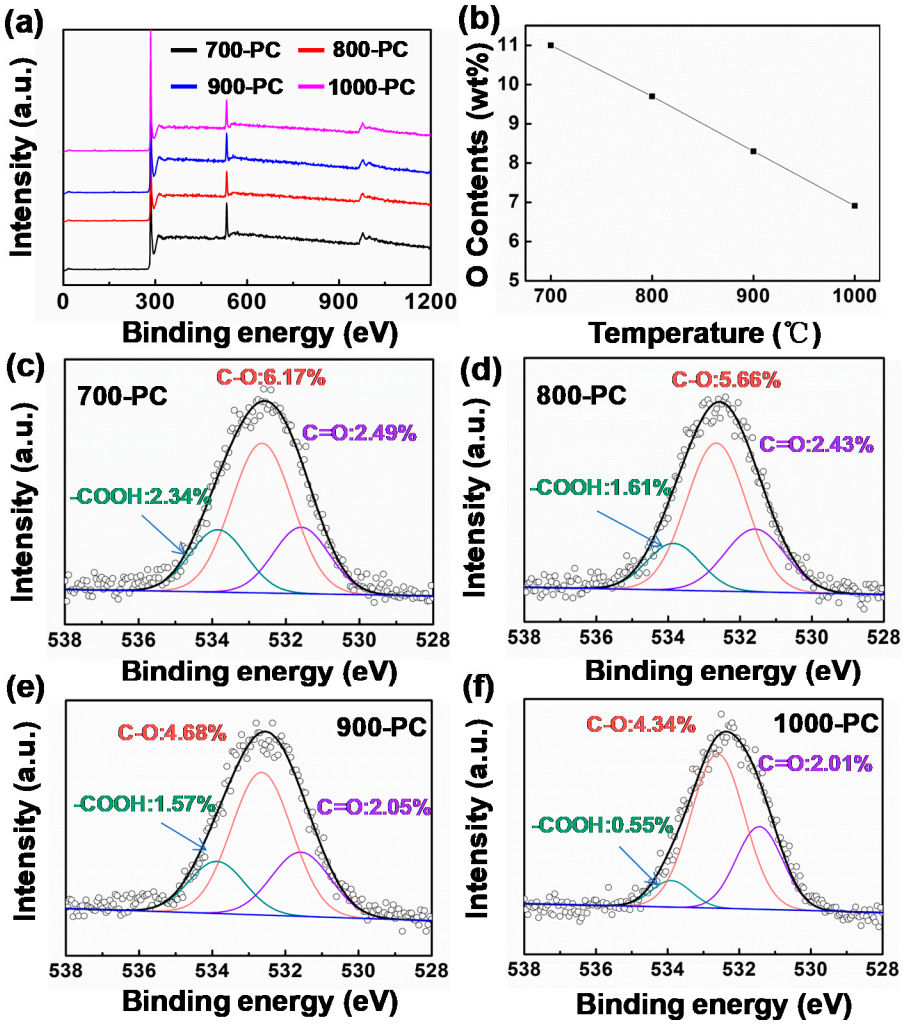

Figure S1. XPS results of PC materials (**a**), Relationships between the O contents and carbonation temperatures (**b**). The contents of C-O, C=O and -COOH groups in PC materials (c-f).

Table S1. Fitted O 1s XPS results for PC samples.

Samples	C=O (at.%)	Position （eV）	C-O (at.%)	Position (eV)	-COOH (at.%)	Position (eV)
700-PC	2.49	531.58	6.17	532.65	2.34	533.85
800-PC	2.43	531.58	5.66	532.66	1.61	533.85
900-PC	2.05	531.57	4.68	532.65	1.57	533.87
1000-PC	2.01	531.44	4.34	532.60	0.55	533.89

Table S2. Fitted S2p XPS results for SPC samples.

Samples	S-O (at.%)	Position （eV）	-C-S-C- (at.%)	Position (eV)		C=S (at.%)	Position (eV)
700-SPC	0.59	167.51	2.51	163.79	165.01	No	No
800-SPC	1.30	167.49	2.92	163.78	165.00	0.14	162.61
900-SPC	0.98	167.70	1.85	163.75	164.95	0.24	162.60
1000-SPC	0.89	168.12	1.78	163.73	164.90	0.30	162.72

Table S3. Element analysis results of PC and SPC materials.

Samples	**N wt%**	**C wt%**	**H wt%**	**S wt%**	**O wt%**
700-PC	1.11	88.42	0.43	0.67	9.37
800-PC	1.11	89.22	0.38	0.72	8.57
900-PC	1.04	89.55	0.34	0.83	8.24
1000-PC	0.98	91.02	0.30	0.09	7.61
700-SPC	0.99	77.67	1.32	14.88	5.13
800-SPC	0.98	77.92	1.41	14.98	4.72
900-SPC	0.86	79.15	0.74	12.16	7.09
1000-SPC	0.52	83.39	0.34	11.17	4.58

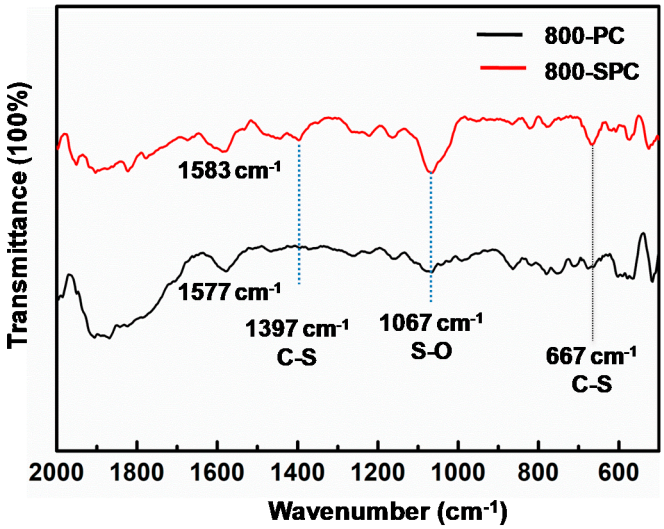

Figure S2. FT-IR results of PC and SPC materials.

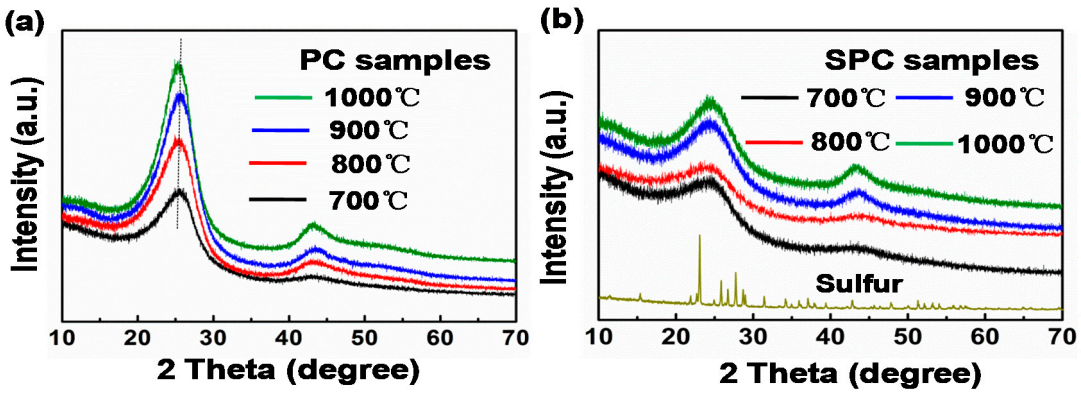

Figure S3. Investigations about the influence of temperature on the structures of PC (**a**) and SPC (**b**) materials by XRD measurements.

Table S4. The calculation results of R values.

Samples	R values	Samples	R values
700-PC	2.42	700-SPC	1.67
800-PC	3.16	800-SPC	1.58
900-PC	3.80	900-SPC	1.78
1000-PC	4.60	1000-SPC	1.86

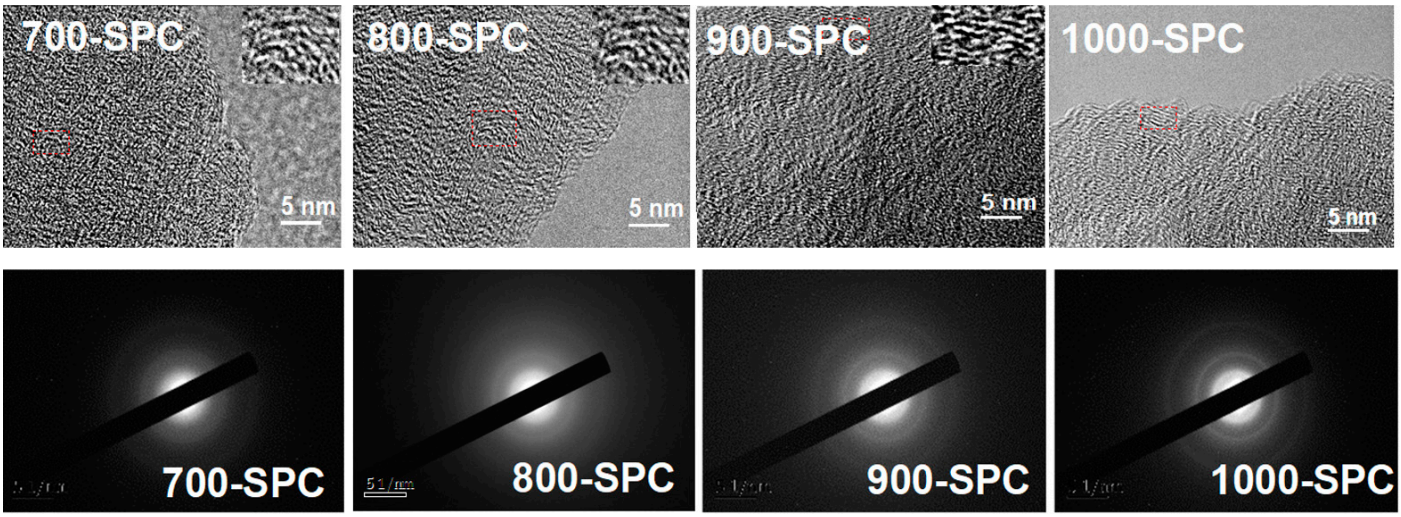

Figure S4. TEM images and selected area electron diffraction (SAED) patterns of PC materials.

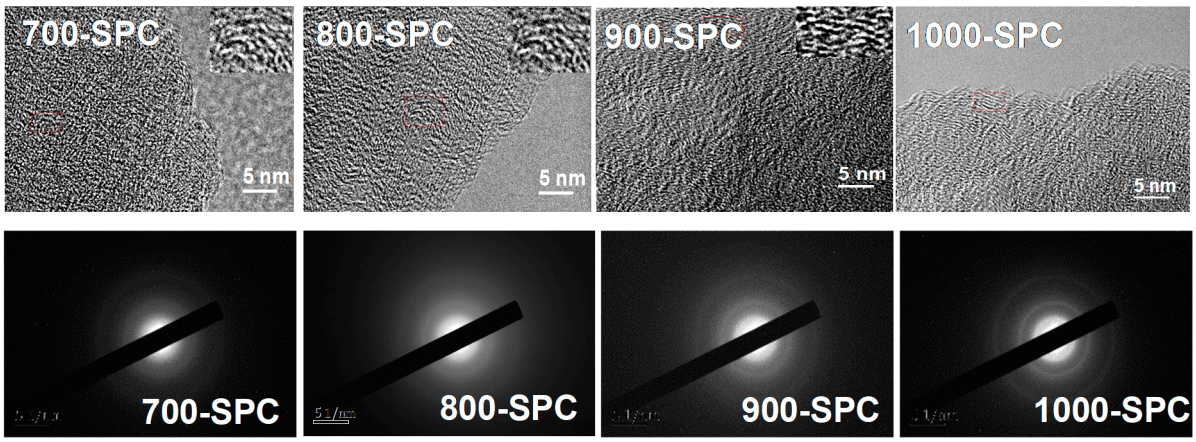

Figure S5. TEM images and selected area electron diffraction (SAED) patterns of SPC materials.

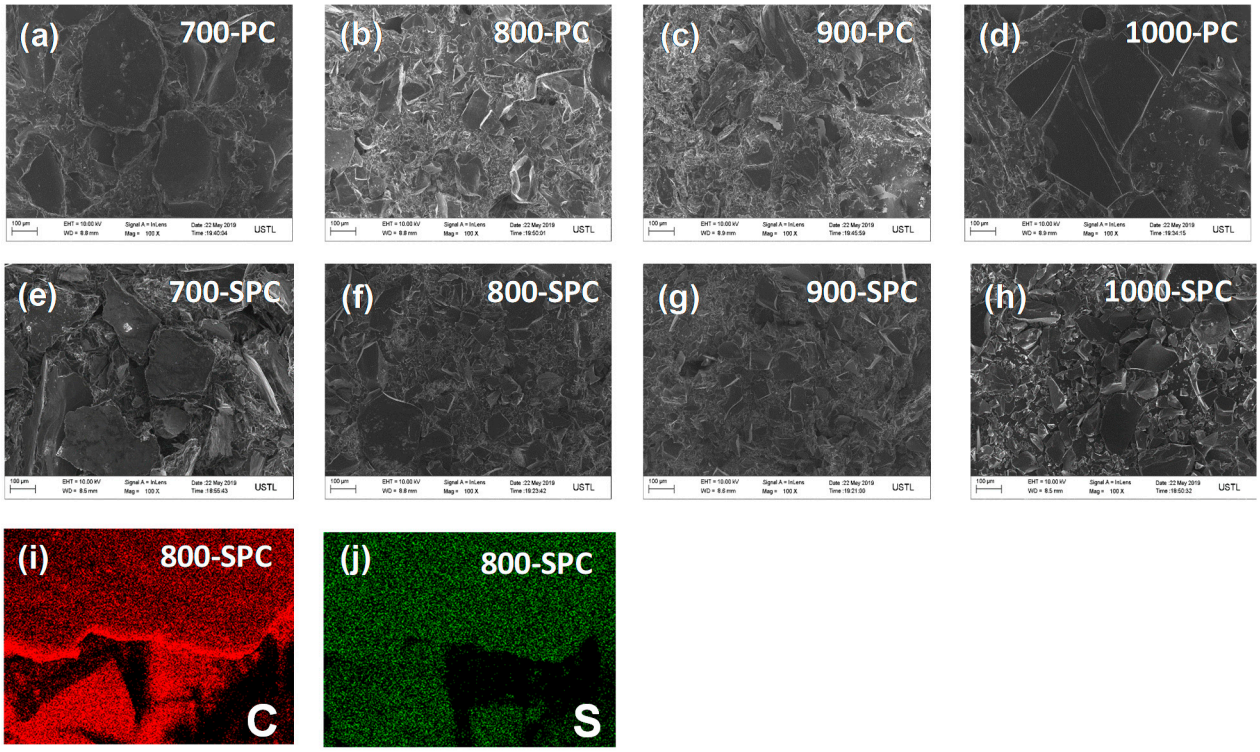

Figure S6. SEM morphologies of PC (**a**–**d**) and SPC (**e**–**h**) materials, and EDS mapping of (**i**) C, and (**j**) S.

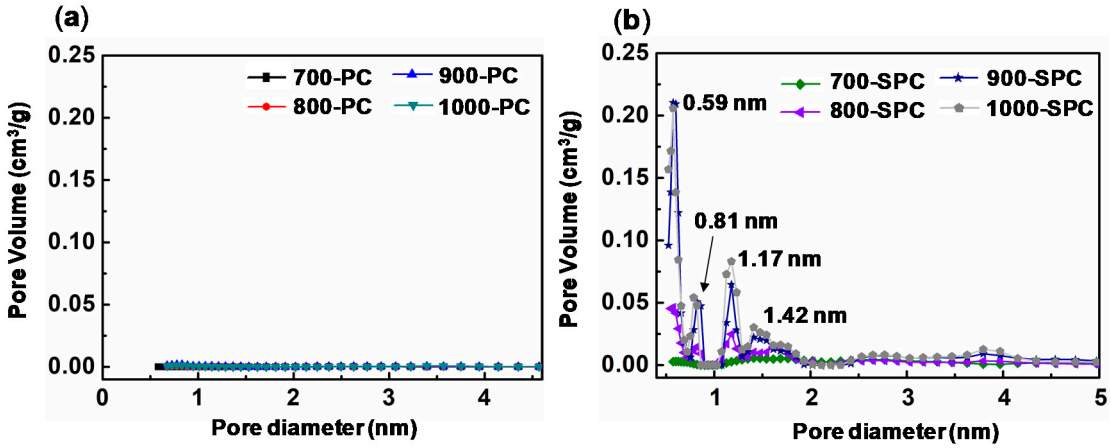

Figure S7. Pore size distribution curves of PC (**a**) and SPC (**b**) materials.

Table S5. Characteristic parameters about structures and specific surface areas of materials. S_{BET}=total BET surface area; V_{total}= total pore volume.

Samples	S_{BET} ($m^2 \cdot g^{-1}$)	V_{total} ($cm^3 \cdot g^{-1}$)
700-PC	0.495	0.00192
800-PC	1.788	0.00220
900-PC	3.642	0.00492
1000-PC	2.663	0.00623
700-SPC	20.642	0.01801
800-SPC	50.940	0.03450
900-SPC	143.959	0.08337
1000-SPC	180.280	0.01099

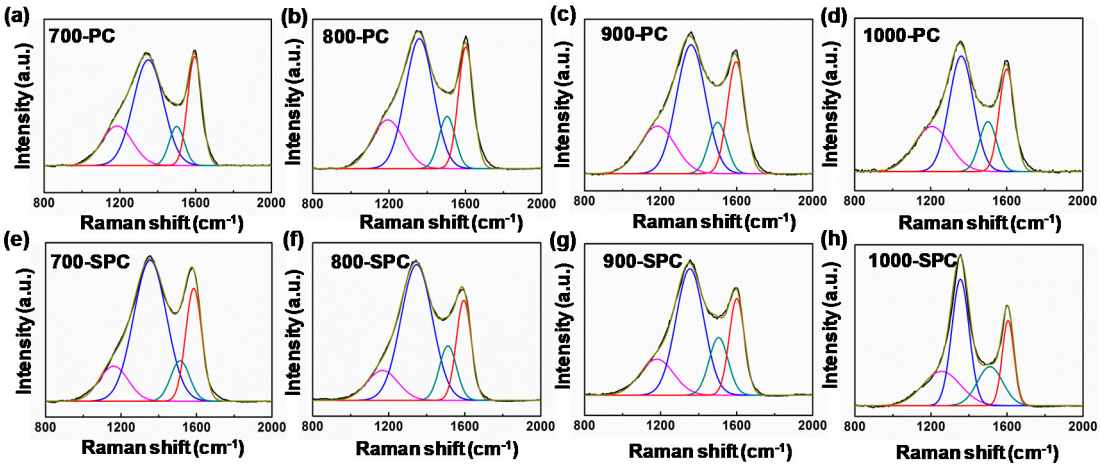

Figure S8. Raman results of PC and SPC materials.

Table S6. Fitted data from Raman results.

Samples	I_D/I_G	L_a (nm)	Samples	I_D/I_G	L_a (nm)
700-PC	2.04	9.40	700-SPC	2.55	7.54
800-PC	1.98	9.71	800-SPC	2.86	6.72
900-PC	1.89	10.17	900-SPC	2.39	8.04
1000-PC	1.82	10.56	1000-SPC	2.18	8.82

L_a (nm) = $(2.4 \times 10^{-10}) \times \lambda_{nm}^{4} \times (I_G/I_D)$ [1], λ_{nm}: Laser Wavelength (532 nm).

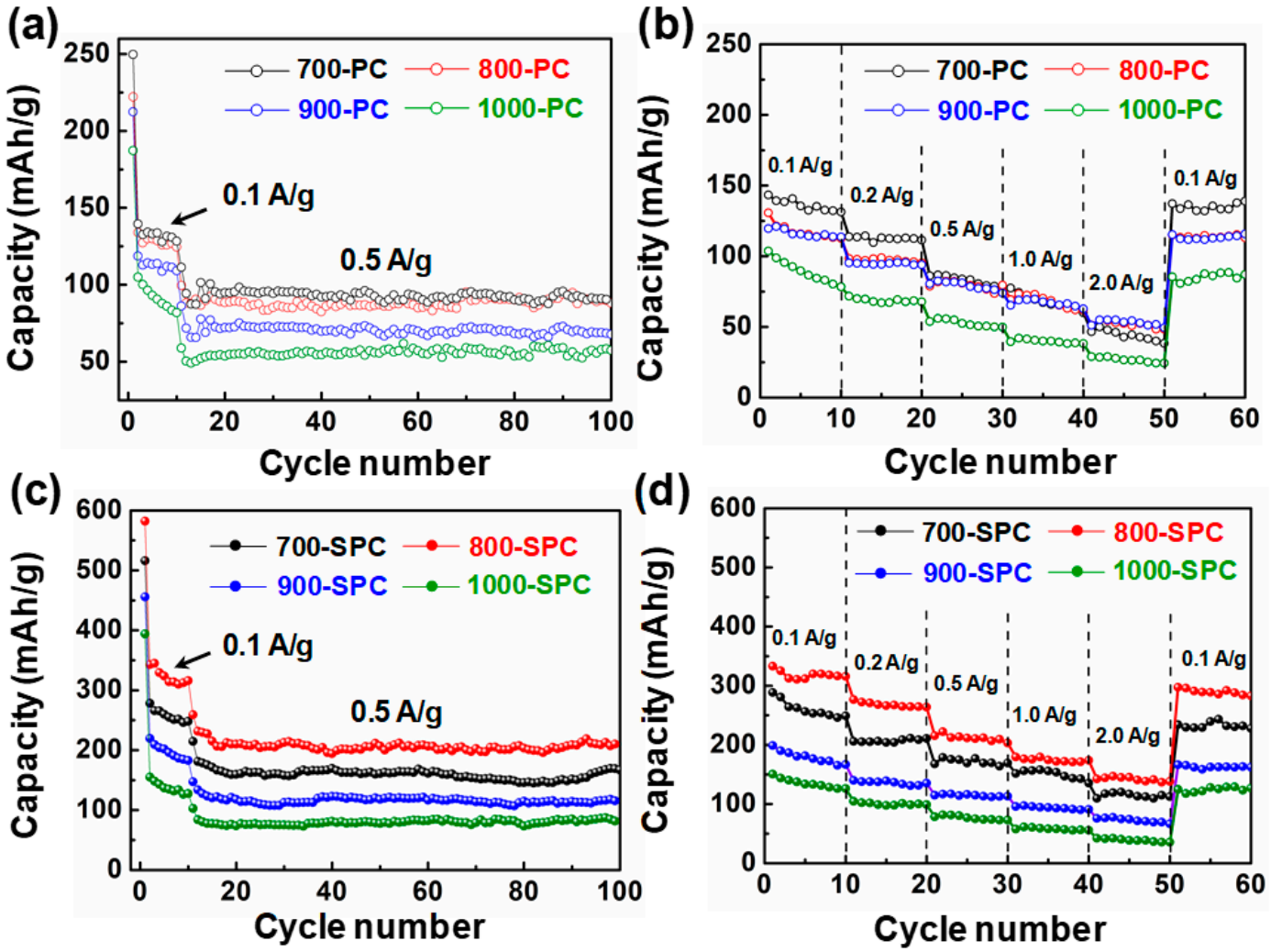

Figure S9. Cycling performances of PC materials (**a**), Rate performances of PC materials (**b**), Cycling performances of SPC materials (**c**) and rate performances of SPC materials (**d**).

Table S7. Comparisons of lithium storage properties of 800-SPC and other carbon materials in previous work.

Materials	Cycle Ability	Rate Capability (mAh/g)	References
pitch-based carbon	80.2% after 2000 cycles at 2000 mA/g	333 at 100 mA/g 215 at 500 mA/g 142 at 2000 mA/g	This work
Carbonized-leaf	90% after 200 Cycles at 40 mA/g	320 at 20 mA/g 270 at 40 mA/g	[2]
Carbonized okara	stable at 1688 mA/g for 2000 cycles	302 at 37.5 mA/g 32 at 7.5 A g	[3]
Carbonized cotton	97% after 100 Cycles at 30 mA/g	275 at 150 mA/g 180 at 300 mA/g	[4]
Carbon nanoparticles prepared from coconut oil	71.2% after 50 Cycles at 100 mA/g	135 at 200 mA/g 107 at 400 mA/g	[5]
Carbonized banana peel	78% after 300 Cycles at 100 mA/g	325 at 100 mA/g 75 at 5000 mA/g	[6]
Carbonized polyvinyl chloride nanofibers	stable after 150 cycles at 12 mA/g	194 at 60 mA/g 147 at 240 mA/g	[7]
Carbonized pine pollen	98% after 200 cycles at 200mA/g	236 at 100 mA/g 118 at 2 A/g	[8]

Mesoporous soft carbon prepared from mesophase pitch	stable after 3000 cycles at 500 mA/g	105 at 500 mA/g 90 at 2000 mA/g	[9]
Pitch-based Carbon	70% after 500 cycles at 400 mA/g	189 at 400 mA/g 137 at 2000 mA/g	[1]
Carbon prepared by coal tar pitch with salt template method	93.4 % after 1000 cycles at 2000 mA/g	272 at 100 mA/g 186 at 500 mA/g	[10]
MCMBs carbonized at 700°C	83% after 50 cycles at 15 mA/g	232 at 25 mA/g 111 at 200 mA/g	[11]
Hard-soft carbon composite produced from biomass and oil waste	74% after 100 cycles at 150 mA/g	250 at 60 mA/g 75 at 1200 mA/g	[12]

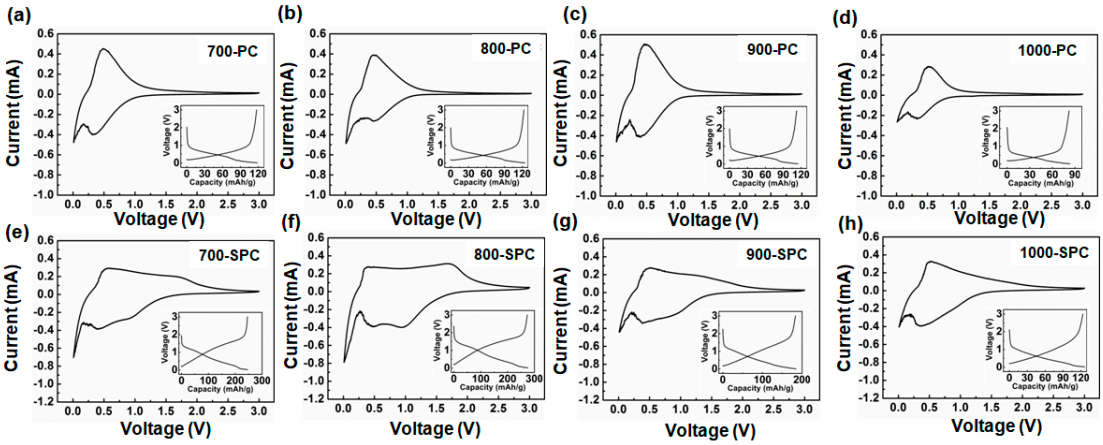

Figure S10. CV profiles of PC materials (**a**–**d**) and SPC materials of (**e**–**h**) at scan rate of 0.5 mV/s. The charge-discharge measurement results of PC materials (**a**–**d**) and SPC materials of (**e**–**h**) are inserted into CV profiles.

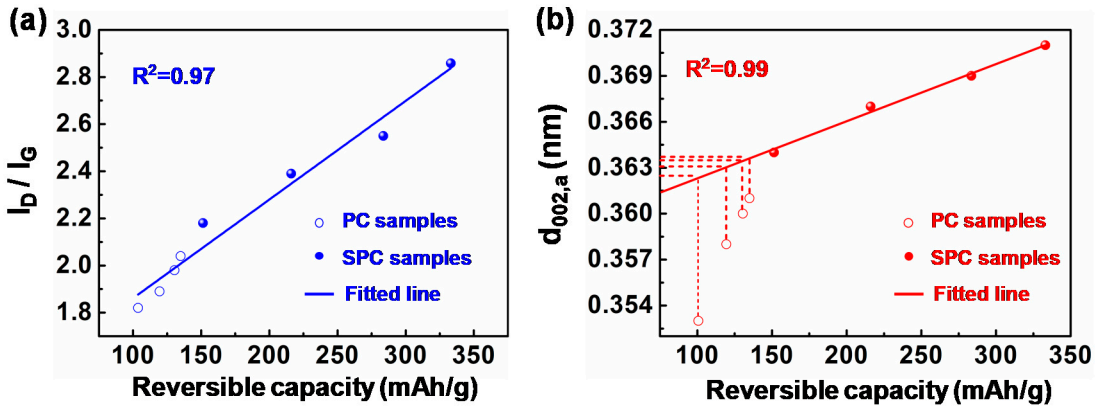

Figure S11. Illustrations of relationships of I_D/I_G and $d_{002,a}$ with reversible capacity.

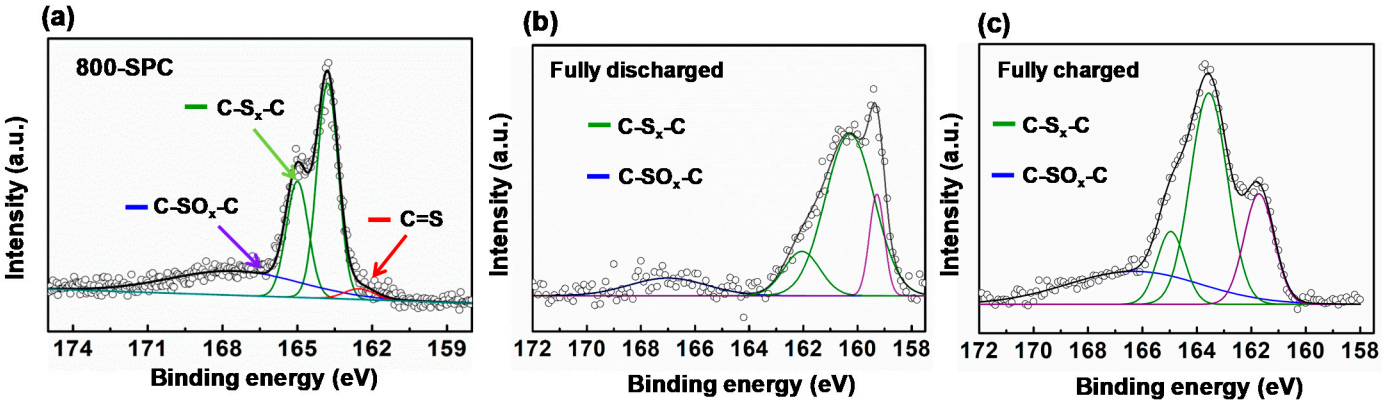

Figure S12. XPS results of 800-SPC (**a**), fully discharged 800-SPC (**b**) and fully charged 800-SPC (**c**).

Table S8. Conversions of binding energies of 800-SPC, fully discharged 800-SPC and fully charged 800-SPC.

S-containing Groups	Characteristic binding energies of 800-SPC (eV)	Binding energies of fully discharged 800-SPC (eV)	Binding energies of fully charged 800-SPC (eV)
–C-S$_x$-C	163.8 and 165.0	160.5 and 162.1	163.3 and 164.8
–C-SO$_x$-C	167.5	167.0	166.4

References

1. Qi, Y.R.; Lu, Y.X.; Ding, F.X.; Zhang, Q.Q.; Li, H.; Huang, X.J.; Chen, L.Q.; Hu, Y.S. Slope-dominated carbon anode with high specific capacity and superior rate capability for high safety Na-ion batteries. *Angew. Chem. Int. Ed.* **2019**, *58*, 4361-4365.
2. Li, H.B.; Shen, F.; Luo, W.; Dai, J.Q.; Han, X.G.; Chen, Y.N.; Yao, Y.G.; Fu, K.; Zhu, H.L.; Hitz, E.M.; Hu, L.B. Carbonized-leaf membrane with anisotropic surfaces for sodium-ion battery. *ACS Appl. Mater. Interfaces.* **2016**, *8*, 2204-2210.
3. Yang, T. Z.; Qian, T.; Wang, M.F.; Shen, X.W.; Xu, N.; Sun, Z.Z.; Yan, C.L. A Sustainable route from biomass byproduct okara to high content nitrogen-doped carbon sheets for efficient sodium ion batteries. *Adv. Mater.* **2016**, *28*, 539-545.
4. Li, Y.M.; Hu, Y-S; Titirici, M-M; Chen, L.Q.; Huang, X.J. Hard carbon microtubesmade from renewable cotton as high-performance anode material for sodium-ion batteries. *Adv. Energy Mater.* **2016**, *6*, 1600659.
5. Gaddam, R.R.; Yang, D.F.; Narayan, R.; Raju, K.; Kumar, N.A.; Zhao, X.S. Biomass derived carbon nanoparticleas anodes for high performance sodium and lithium ion batteries. *Nano Energy.* **2016**, *26*, 346-352.
6. Lotfabad, E.M.; Ding, J.; Cui, K.; Kohandehghan, A.; Kalisvaart, W.P.; Hazelton, M.; Mitlin, D. High-density sodium and lithium ion battery anodes from banana peels. *ACS Nano.* **2014**, *8*, 7115-7129.
7. Bai, Y.; Wang, Z.; Wu, C.; Xu, R.; Wu, F.; Liu, Y. C.; Li, H.; Li, Y.; Lu, J.; Amine, K. Hard carbon originated from polyvinyl chloride nanofibers as high-performance anode material for Na-ion battery. *ACS Appl. Mater. Interfaces.* **2015**, *7*, 5598-5604.
8. Zhang, Y.; Li, X.; Dong, P.; Wu, G.; Xiao, J.; Zeng, X.; Zhang, Y.; Sun, X. Honeycomb-like hard carbon derived from pine pollen as high-performance anode material for sodium-ion batteries. *ACS Appl. Mater. Interfaces.* **2018**, *10*, 42796-42803.
9. Cao, B.; Liu, H.; Xu, B.; Lei, Y.F.; Chen, X.H.; Song, H.H. Mesoporous soft carbon as an anode material for sodium ion batteries with superior rate and cycling performance. *J. Mater. Chem. A.* **2016**, *4*, 6472-6478.
10. Wang, Y.W.; Xiao, N.; Wang, Z.Y.; Li, H. J.; Yu, M.L.; Tang, Y.C.; Hao, M.Y.; Liu, C.; Zhou, Y.; Qiu, J.S. Rational design of high-performance sodium-ion battery anode by molecular engineering of coal tar pitch. *Chem. Eng. J.* **2018**, *342*, 52-60.
11. Song, L.J.; Liu, S.S.; Yu, B.J.; Wang, C.Y.; Li, M.W. Anode performance of mesocarbonmicrobeads for sodium-ion batteries. *Carbon.* **2015**, *95*, 972-977.
12. Xie, F.; Xu, Z.; Jensen, A.C.S.; Au, H.; Lu, Y.; Araullo-Peters, V.; Drew, A.J.; Hu, Y.S.; Titirici, M.M. Hard-Soft carbon composite anodes with synergistic sodium storage performance. *Adv. Funct. Mater.* **2019**, *29*, 1901072.